Journal of Nanobiotechnology

RESEARCH

Open Access

Multi-omics analyses reveal the responses of wheat (*Triticum aestivum* L.) and rhizosphere bacterial community to nano(micro)plastics stress

Ming Zhuang[1], Chengkui Qiao[2,3*], Lijun Han[1*], Yingying Bi[4], Mengyuan Cao[1], Shiyu Wang[1], Linlin Guo[2], Rongli Pang[2] and Hanzhong Xie[2]

Abstract

The pervasive existence of nanoplastics (NPs) and microplastics (MPs) in soil has become a worldwide environmental concern. N/MPs exist in the environment in a variety of forms, sizes, and concentrations, while multi-omics studies on the comprehensive impact of N/MPs with different properties (e.g. type and size) on plants remain limited. Therefore, this study utilized multi-omics analysis methods to investigate the effects of three common polymers [polyethylene-NPs (PE-NPs, 50 nm), PE-MPs (PE-MPs, 10 μm), and polystyrene-MPs (PS-MPs, 10 μm)] on the growth and stress response of wheat, as well as the rhizosphere microbial community at two concentrations (0.05 and 0.5 g/kg). PS and PE exhibited different effects for the same particle size and concentration. PE-NPs had the most severe stress effects, resulting in reduced rhizosphere bacteria diversity, plant biomass, and antioxidant enzyme activity while increasing beneficial bacteria richness. N/MPs altered the expression of nitrogen-, phosphorus-, and sulfur-related functional genes in rhizosphere bacteria, thereby affecting photosynthesis, as well as metabolite and gene levels in wheat leaves. Partial least squares pathway models (PLSPMs) indicated that concentration, size, and type play important roles in the impact of N/MPs on the plant ecological environment, which could have essential implications for assessing the environmental risk of N/MPs.

Keywords Nanoplastics, Wheat, Rhizosphere soil bacteria, Metabolomic, Transcriptome

*Correspondence:
Chengkui Qiao
qiaochengkui@caas.cn
Lijun Han
hlj2000@cau.edu.cn
Full list of author information is available at the end of the article

Graphical Abstract

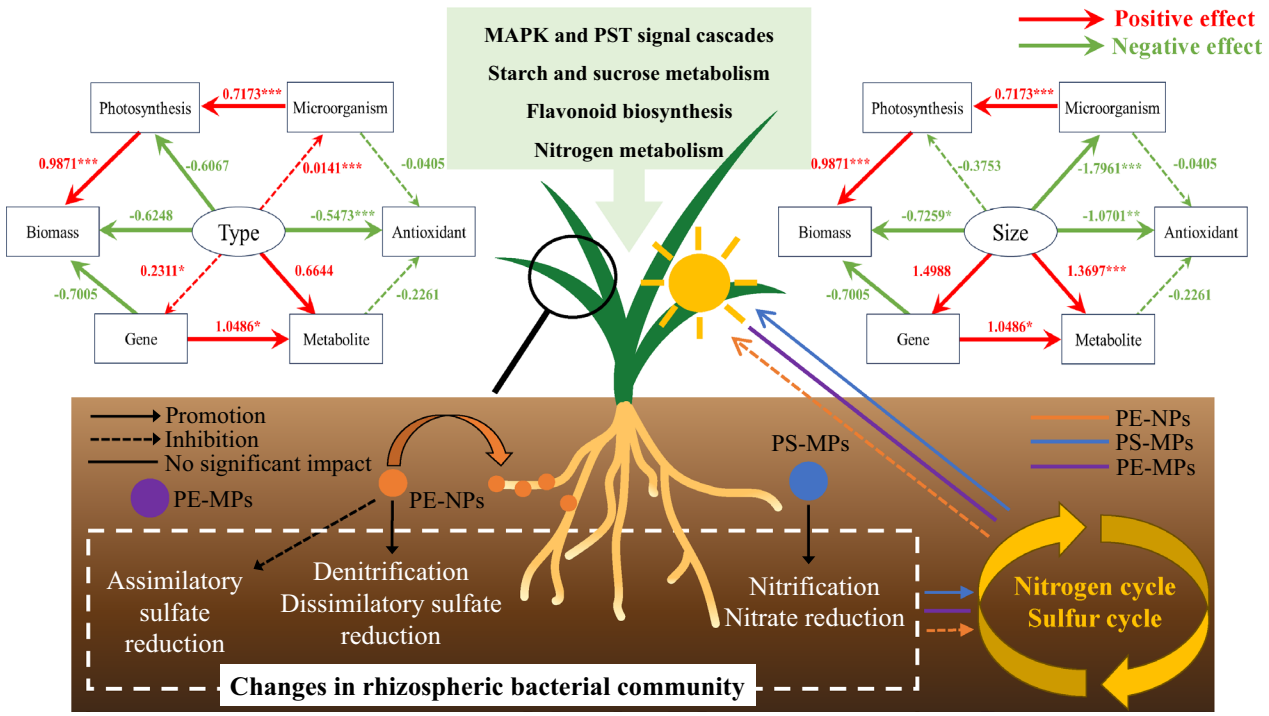

Introduction

The widespread and long-term use of plastics in daily life has led to a significant environmental challenge [1]. Large plastic objects degrade into smaller particles through microbial decomposition, exposure to UV light, and mechanical wear. These plastic fragments are typically categorized into two groups based on their size: microplastics (MPs, < 5 mm) and nanoplastics (NPs, < 100 nm) [2]. Compared to MPs, NPs have a smaller size and a greater specific surface area, which facilitates cellular penetration and makes them more likely to enter root tissue via intercellular routes or crack-entry modes [3]. This enables them to accumulate in plants and cause biological toxicity [4, 5], highlighting NPs as an increasingly significant global contaminant [6]. Plastic degradation and fragmentation on land surfaces occur more extensively than in aquatic systems, resulting in a relatively high quantity of N/MPs in terrestrial systems. Among them, agricultural soils might suffer the most serious N/MP pollution due to widespread use of sewage, sludge, and plastic mulches [7]. Therefore, the toxicological impacts of N/MPs on the agricultural ecosystem may be higher than those on other environments [3].

An increasing body of research suggests that N/MPs may affect the physicochemical characteristics of soil, destabilizing its structure and quality, and potentially disrupting soil ecosystems and species. For example, N/MPs can affect soil chemical parameters, and modify physical soil characteristics, including bulk density, porosity, structure, and water-holding capacity [3]. Additionally, this disturbance would affect the structure and activity of soil microbial communities, which are highly sensitive to soil structure [8]. Considering the sensitivity of soil microbial communities to soil structure, this damage will also affect their activity and structure. Several studies indicate that N/MPs can alter the quantity and diversity of bacterial communities [9]; nevertheless, the effects of N/MPs vary depending on factors such as particle type, dosage, and size. For instance, PE had a significant impact on the microbial community compared to PVC. Regarding concentration, the presence of 5% PVC, as opposed to 1%, significantly decreased the abundance of the *Sphingomonadaceae* family, potentially inhibiting the degradation of soil exogenous substances [7]. In the barley seedling experiment, it was found that PS-MPs increased the variety of the root endophytic bacterial population, while PS-NPs decreased the richness and diversity of the fungal community [10].

N/MPs also adversely affect the health, growth, and performance of higher plants [11]. For example, plant biomass, photosynthetic capacity, and plant mass of rape seedlings were significantly decreased with the exposure to PS-NPs [12]. Lian et al. found that PS-NPs significantly altered carbon metabolism, amino acid biosynthesis, plant hormone signal transduction, and plant-pathogen interaction pathways in hydroponically grown wheat [13]. The effects of N/MPs on plant growth metrics may vary depending on their type and/or size [14]. For instance, the impact of low-density polyethylene (LDPE) on the root weight and chlorophyll (Chl) content of lettuce was found to be influenced by its shape [15]. Hence, when evaluating the effects of microplastics on terrestrial plants, it is essential to account for the variations resulting from their types, sizes, and concentrations. Although these findings provide some insights into the toxic mechanisms of MPs on plants, there remains a significant knowledge gap regarding the molecular intricacies that link gene expression, metabolic changes, and physiochemical alterations.

Wheat (Triticum aestivum L.) occupies a prominent position as a primary cereal crop and serves as a fundamental food source for over half of the global population [16]. Moreover, it is widely recognized as one of the most frequently used plant indicators for assessing the potential ecological impacts of nanomaterials [17]. Dhevagi et al. reported that N/MPs are widely present in wheat fields [18]. N/MPs have been found to accumulate along the wheat root xylem cell walls and in the xylem vessel members, inducing photosynthetic impairment and oxidative damage in wheat seedlings [19]. Therefore, it is necessary to study the potential ecological risks of N/MPs on wheat. This greenhouse pot experiment was conducted to explore the integrated alterations in the physiology, biochemistry, antioxidant system, metabolome, and transcriptome of wheat plants, along with the structure and functional genes of the rhizosphere soil bacterial community under N/MPs stress. We selected three common N/MPs in wheat planting fields and compared their comprehensive effects on the wheat-soil system using multi-omics methods. Additionally, we preliminarily explored whether type (PE-MPs vs PS-MPs) and size (PE-MPs vs PE-NPs) factors play different roles in the overall impact of MPs on the wheat-soil system.

Material and methods

Preparation and properties of the materials

Chemicals

PE-N/MPs (10 μm and 50 nm, 0.85 g/cm^3) and PS-MPs (10 μm, 1.05 g/cm^3) were obtained from Jiangsu Sinoma Plasticizing Company (Jiangsu, China). The particle size of all N/MPs was measured using scanning electron microscopy (SEM, ZEISS Gemini 300, Germany) (Fig. S1). Ultrapure water was produced using a Milli-Q water purification system (Millipore, Billerica, MA, USA). All other reagents adhered to HPLC grade standards.

Tested wheat and soil

The wheat variety used was Zhengmai 379. Seeds were sterilized with 3% (v/v) H_2O_2 for 30 min and then thoroughly rinsed with distilled water before use. After selecting seeds of uniform size, they were germinated in seedling trays under dark and moist conditions until the seedlings reached a length of 3–4 mm.

The experimental soil was collected from the top 0–20 cm soil layer of a field in Zhengzhou City, Henan Province, China (34°20′ N, 112°50′ E). Prior to use, soil samples were thoroughly mixed, air-dried, and passed through a 2 mm sieve. The pH of the soil was 5.94, with an organic matter content of 14.3 g kg^{-1} and a cation exchange capacity of 14.8 cmol $^{(+)}$/kg. No plastic particles or debris were found in the soil.

Greenhouse experiment

The experiment took place in a greenhouse at the Zhengzhou Fruit Research Institute, Chinese Academy of Agricultural Sciences. Clean yellow–brown soil was divided into seven portions, each weighing 1 kg. One portion served as the control group (CK). The remaining six portions of soil were mixed separately with PE and PS at concentrations of 0.05 and 0.5 g/kg. PE was available in two particle sizes: 10 μm and 50 nm. These mixtures were labeled as follows: PE-MPs-0.05, PE-MPs-0.5, PE-NPs-0.05, PE-NPs-0.5, PS-MPs-0.05, and PS-MPs-0.5. Each treatment was replicated six times. The test concentrations of MPs were determined based on literature reviews [20]. After thoroughly mixing the soil with the MPs or NPs in each pot, water was added to maintain a water-holding capacity of 60% for 48 h. Fifteen germinated wheat seeds were planted one centimeter deep in each container. The seedling stage of wheat is a critical period for promoting root growth and nurturing robust seedlings, as well as for ensuring the healthy development of subsequent plants [21]. Therefore, before collecting the samples, the pots were kept in a greenhouse for 30 days under controlled conditions: 14 h of light and 8 h of darkness, light intensity of 600 μmol/(m^{2}s), and day and night temperatures of 25/20 °C, with 60% relative humidity.

Sample collection and measurements

Sample collection

Wheat plants were carefully removed from the pots and then separated into shoots and roots using scissors. After retrieving rhizosphere soil from the roots, they

were thoroughly rinsed with tap water, then rinsed several times with distilled water, and finally wiped dry to remove surface moisture. The length and fresh weight of above-ground leaves and roots were promptly measured using a steel ruler and an analytical balance, respectively. The collected plants and soil samples were stored at − 80 °C for subsequent experiments.

Observation of root cell ultrastructure

Wheat roots were submerged in a pre-chilled Petri dish containing 2.5% glutaraldehyde and then cut into 0.3 × 0.3 mm slices using a sharp blade. Following this, the gas was evacuated until the tissue was completely submerged in the fixing solution. Transmission electron microscopy (TEM) analysis of the root cell ultrastructure was performed by Wuhan Servicebio Technology Co., Ltd. (Wuhan, China). The distribution of carbon and other elements on the surface of fresh wheat roots was analyzed using scanning electron microscopy and energy dispersive spectroscopy (SEM–EDS) (AZtecLive Ultim Max 100, UK).

Physiological and biochemical index measurement

Various photosynthesis parameters including water use efficiency (WUE), stomatal conductance (Gs), transpiration (Tr), internal CO_2 concentration (Ci), net photosynthesis rate (Pn), initial fluorescence (Fo), linear electron transfer rate (ETR), photochemical quenching coefficient (qP), maximal photochemical quantum yield (Fv/Fm), actual photochemical efficiency (ΦPSII), and potential activity (Fm), as well as total acid, total flavonoid, soluble sugar content, and antioxidant indicators (malondialdehyde (MDA), superoxide dismutase (SOD), peroxidase (POD), and catalase (CAT)) of wheat were determined. Detailed procedures are provided in Texts S1, S2, and S3 of the Supporting Information (SI).

Metabolomic analysis

Ultra-high-performance liquid chromatography with quadrupole-time of flight mass spectrometry (UHPLC-Q-TOF-MS, AB Sciex, USA) was utilized to analyze primary and secondary metabolites in an untargeted manner. Additionally, UHPLC-MS/MS (Agilent, USA) was used to quantify the specific differential compounds (detailed parameters are in Text S4 and Table S1 of the SI). Detailed pretreatment process is provided Text S5.

Transcriptome determination

The cDNA libraries were sequenced on the Illumina sequencing platform by Metware Biotechnology Co., Ltd. (Wuhan, China). RNA extracted from wheat leaves was sequenced, and after screening raw data, the sequencing error rate and GC content distribution were examined to obtain clean reads for further analysis. The expression levels of transcripts or genes were quantified using FPKM (fragments per kilobase per million) values.

Rhizosphere soil bacterial diversity, taxonomic and functional analysis

High-throughput sequencing of the soil bacterial 16S rRNA gene was performed using an Illumina MiSeq platform (Personalbio, Inc., Shanghai, China) to investigate the diversity and composition of the microbial community. Detailed analysis procedure is provided in Text S6.

Statistical analysis

All treatments in this experiment were arranged using a fully randomized approach. In this study, OriginPro 2024 and SPSS 22.0 were utilized for data processing. Normal distribution was assessed using Quantile–Quantile plots and Shapiro–Wilk tests, and homogeneity of variance was evaluated with Levene's test. After the homogeneity of variance condition was met (or after data transformation), one-way analysis of variance (ANOVA) was conducted for each index, followed by post-hoc Duncan tests for multiple comparisons. A P-value of less than 0.05 indicated a significant difference. The partial least squares path model (PLSPM) analysis was conducted using R Studio.

Results

Effect of N/MPs on wheat root cell ultrastructure

Most wheat root cells in the CK treatment group exhibited uniformly distributed contents within the vacuoles, as depicted in Fig. 1. Mitochondria exhibited a full, clear, and structurally complete morphology, tightly organized within the cellular cavity. In contrast, wheat root cells subjected to N/MPs stress exhibited a disrupted cell structure compared to the control, resulting in root cell plasmolysis. PE-MPs induced more severe damage to organelles in root cells than PS-MPs, resulting in disrupted nuclei and turbid vesicles. The extent of damage intensified with the decrease in the particle size of PE. The SEM–EDS electron microscopy revealed a significant enrichment of C and O in wheat roots. Notably, PE-NPs treatment increased the C content in wheat roots while reducing the content of Al and Si. These results suggested that PE-NPs might accumulate in wheat roots, disrupt root cell structure and possibly inhibit or reduce the absorption and accumulation of Al and Si.

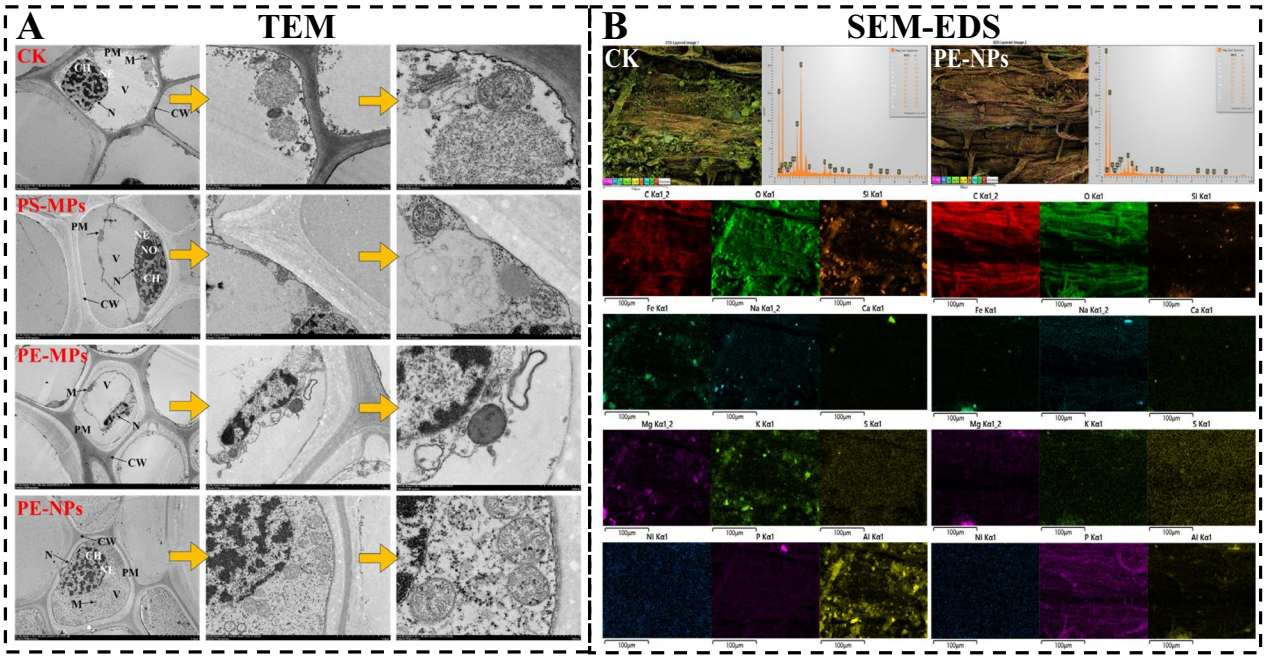

Fig. 1 **A** Ultrastructure of root cells in wheat roots treated with and without N/MPs. The ultrastructure of root cells in wheat roots in the CK, PS-MPs, PE-MPs, and PE-NPs groups. N (nucleus), NO (nucleolus), CH (chromatin), NE (nuclear envelope), V (vacuole), M (mitochondria), P (plastid), S (starch granule), PM (plasma membrane), CW (cell wall) and ER (endoplasmic reticulum); **B** Imaging of different elements on wheat roots through SEM–EDS analysis

Morphological and photosynthetic merits changes and antioxidant system responses of wheat plant after exposure to N/MPs

The effect of various MPs on the shoots, roots, and fresh weight of wheat plants varied: PS-MPs had no significant effect on wheat plant growth, while PE-MPs and PE-NPs exhibited inhibitory effects (Fig. 2A, B). The treatment of PE-NPs at 0.5 g/kg led to a significant decrease in shoot length and fresh weights of both shoot and root, which were 13, 10, 19, and 16% lower than the CK treatment ($p < 0.05$), respectively. Similarly, the content of soluble sugar, total acid, and total flavonoids in wheat plants was more significantly affected by PE than by PS, although it exhibited a gradual increase with decreasing particle size. Wheat leaves subjected to PE-NPs-0.5 treatment exhibited the highest levels of soluble sugar, total acid, and total flavonoids, which were 91, 25, and 11% higher than those in the CK, respectively (Fig. 2C).

Figure 3 illustrated the effects of N/MPs on antioxidant system responsed in leaves and roots of wheat. PS-MPs and PE-MPs-0.05 treatment did not significantly affect the antioxidant system of wheat leaves. For PE, high concentration MPs and low concentration NPs have similar effects on the antioxidant reaction system, resulting in lower MDA content and higher antioxidant enzyme activity (SOD, POD, and CAT) in leaves. However, when the concentration of PE-NPs was increased to 0.5 g/kg, the MDA content was 27% higher than CK, and the activity of SOD, POD, and CAT were all significantly decreased. The trends in MDA content and antioxidant enzyme activities in the roots were consistent with those observed in the leaves (Fig. 3B).

The effects of N/MPs on the photosynthesis parameters of wheat leaves, as illustrated in Fig. 4, showed that wheat plants responded to PS-MPs stress by increasing Pn, Gs, Tr, and WUE levels, while PE-MPs and PE-NPs inhibited these parameters, with a trend of decreasing for the smaller size of PE. The effect of the N/MPs on interstitial Ci was an exception, which was opposite to the above parameters. For the same types of N/MPs, the higher concentration of the N/MPs had a relatively greater impact on the photosynthesis parameters of the leaves. Specifically, PE-NP-0.5 treatment had the lowest values of Pn, Gs, Tr, and WUE, which were 38, 17, 15, and 9% lower than CK, respectively (Fig. 4A). The Chl fluorescence parameters in Fig. 4B showed similar results to those in Fig. 4A. PE significantly inhibited Fv/Fm, qP, ETR, ΦPSII, and Fm, especially NPs. Fo showed the opposite results. The Chl and carotenoid contents also verified the above results (Fig. 4C): the PE-NPs-0.5 treatment significantly reduced the total Chl content, Chl a/b ratio and carotenoid content in wheat leaves.

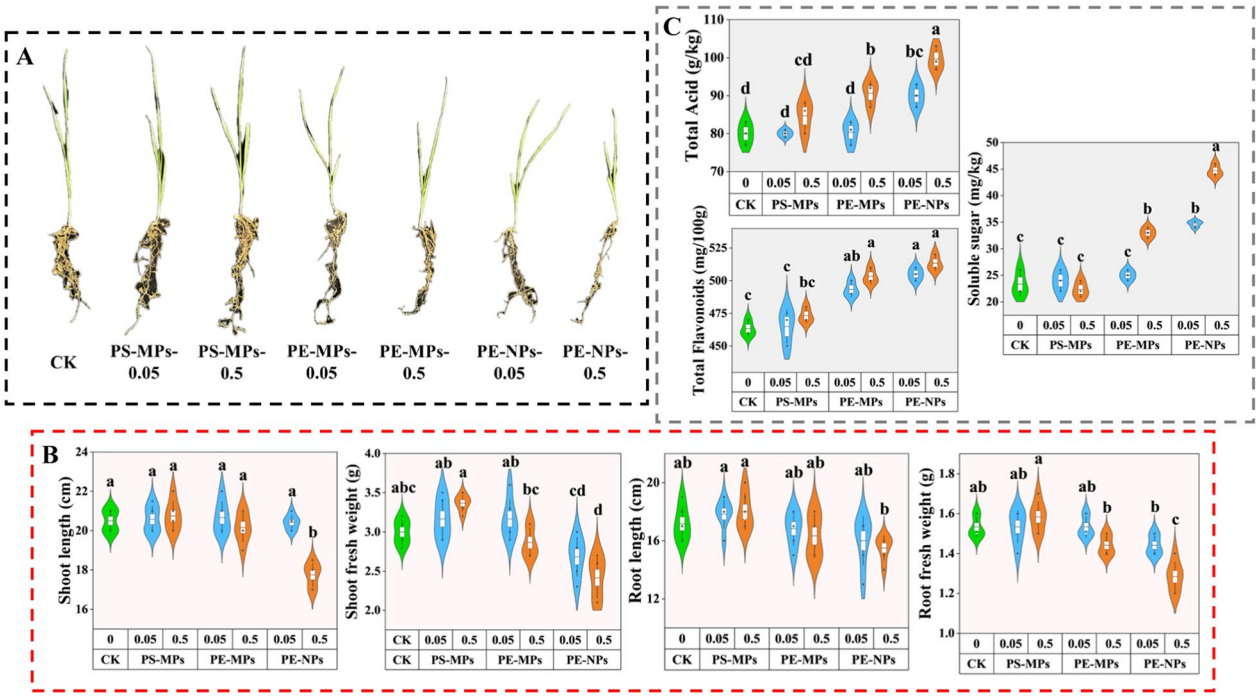

Fig. 2 Effects of N/MPs on (**A**) plant morphology, (**B**) shoot and root biomass, plant height, and root length, (**C**) total acid and flavonoid, and soluble sugar of wheat

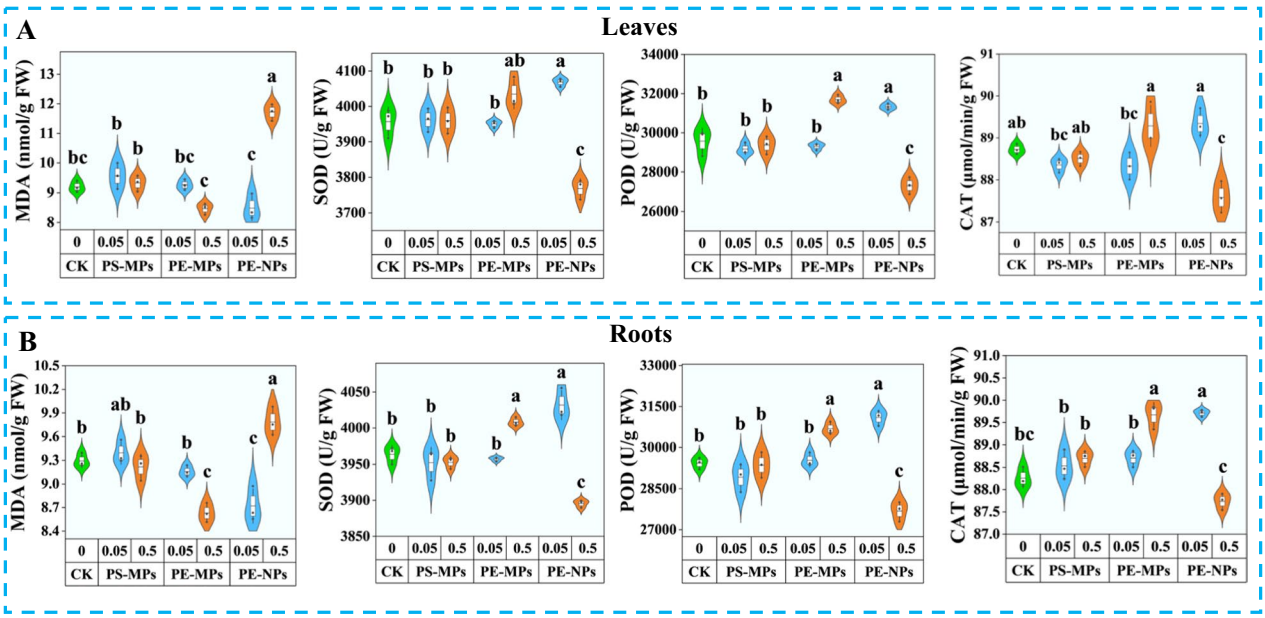

Fig. 3 Effects of N/MPs on antioxidant enzyme (SOD, POD, CAT) activity and MDA content in leaves and roots of wheat

Metabolic responses to N/MPs stress

Principal component analysis (PCA) and hierarchical cluster analysis results revealed similar accumulation trends of metabolites in PE-MPs and PS-MPs in leaves, with the most significant changes observed in the PE-NPs-0.5 group (Fig. 5A, B). The volcano plots (Fig. 5C) showed that the number of differentially accumulated metabolites (DAMs) (|fold change| > 2 and $P < 0.05$) in

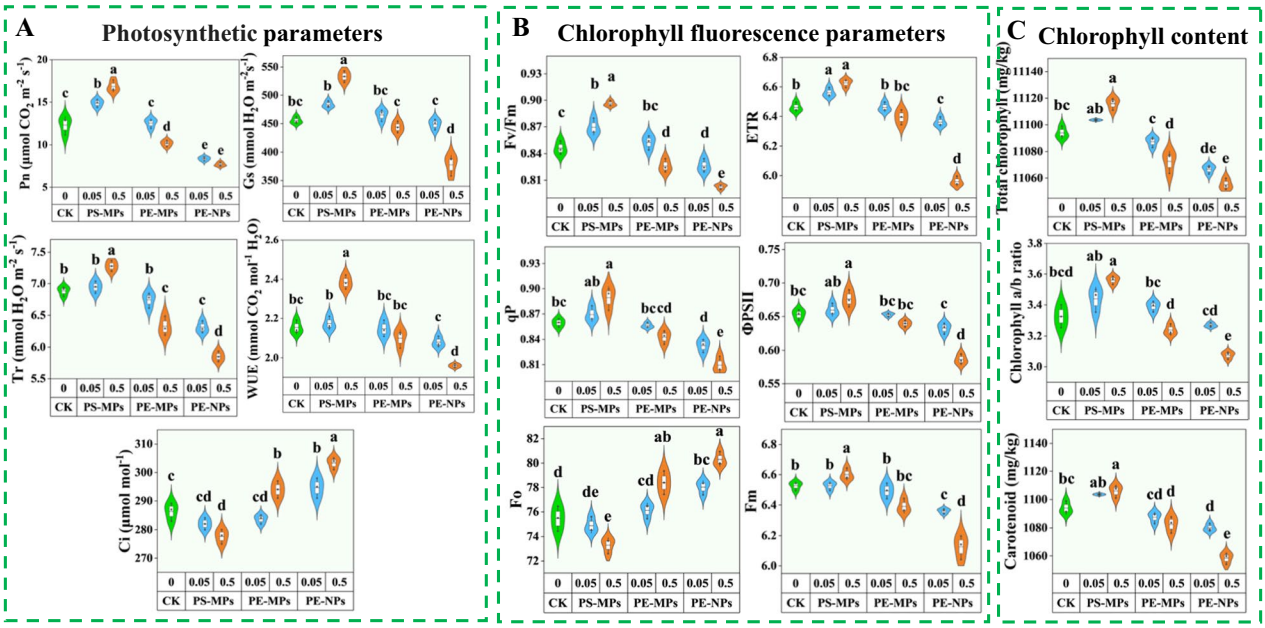

Fig. 4 Effects of N/MPs on photosynthesis of wheat leaves

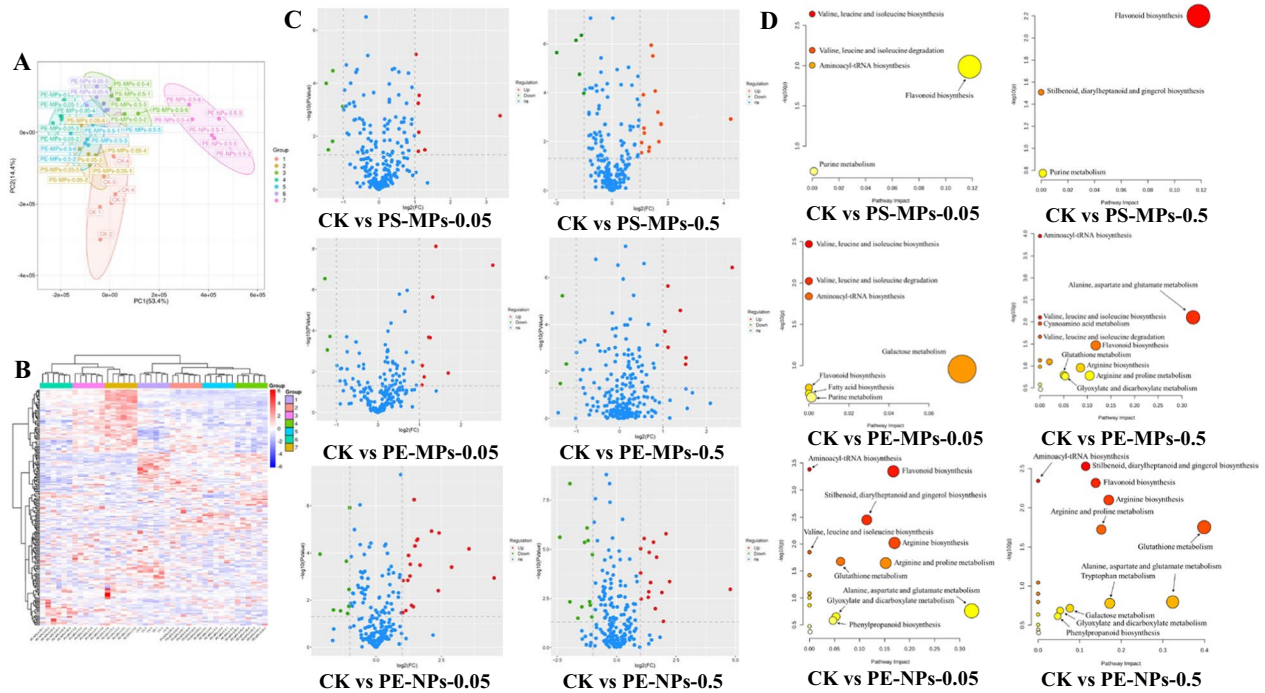

Fig. 5 The distribution of DAMs related to the responses of wheat in leaves after 30 days of N/MPs exposure: **A** PCA of DAMs. **B** Heatmaps of DAMs compared between different groups. **C** Volcano plots displaying the DAMs that are up- and down-regulated. Red plots represent upregulated DAMs; green plots represent downregulated DAMs; blue plots represent metabolites with no significant difference. **D** KEGG pathway enrichment analysis of DAMs

wheat leaves increased with rising doses of N/MPs, suggesting a dosage-dependent effect of N/MPs stress on metabolite expression. For each treatment with PS-MPs, PE-MPs, and PE-NPs, the number of DAMs was

12 (5 down- and 7 up-regulated), 12 (3 down- and 9 up-regulated), and 28 (8 down- and 20 up-regulated) at the dosage of 0.05 g/kg, and it was 19 (5 down- and 14 up-regulated), 9 (3 down- and 6 up-regulated), and 28 (12 down- and 16 up-regulated) at the dosage of 0.5 g/kg, respectively. The DAMs were primarily categorized as amino acids, terpenoids, flavonoids and phenylpropanes. Genes and Genomes (KEGG) pathway enrichment analysis of DAMs results indicated significant alteration of the 'Flavonoid Biosynthesis Pathway' in all N/MPs treatments. For different types of MPs, exposure to PS-MPs had a relatively small impact on wheat plants, with only 3–5 metabolic pathways influenced, while exposure to PE-MPs significantly affected 'Galactose Metabolism', 'Alanine, Aspartate, and Glucose Metabolism', with 7–15 impacted pathways for the different treatment dosages. For the treatment with NPs, it had a significant impact on 16–18 metabolic pathways of wheat, including 'Stilbenoid, Dialylheptanoid, and Ginger Biosynthesis', 'Arginine Biosynthesis', 'Arginine and Proline Metabolism', and 'Glutathione Metabolism' ($p < 0.05$, impact > 0.1) (Fig. 5D).

Transcriptional responses to N/MPs stress

The PCA and cluster heatmap results validated the metabolomics findings. The most significant changes in gene expression in wheat leaves were observed in the PE-NPs group (Fig. 6A, D). Our research revealed significant differentially expressed genes (DEGs) in the PS-MPs, PE-MPs, and PE-NPs groups. Specifically, there were 460 DEGs in the PS-MPs group, with 174 downregulated and 286 upregulated DEGs; 510 downregulated and 421 upregulated genes in the PE-MPs group; and 1899 down-regulated and 1242 up-regulated DEGs in the PE-NPs group (Fig. 6B, E). The specific DEGs numbered 157, 521, and 2688, respectively (Fig. 6C). The results of the gene ontology (GO) enrichment analysis were classified into 24 annotated functional subcategories. From these, the eight GO terms with the lowest q-values among the three GO categories (biological process (BP), cellular component (CC), and molecular function (MF)) were selected. Among them, 'Photosystem II' (GO: 0009523), associated with 497 expressed genes, was the most enriched GO term in the PE-NPs versus CK group. Additionally, 'Chlorophyll Binding' (GO: 0016168) had the

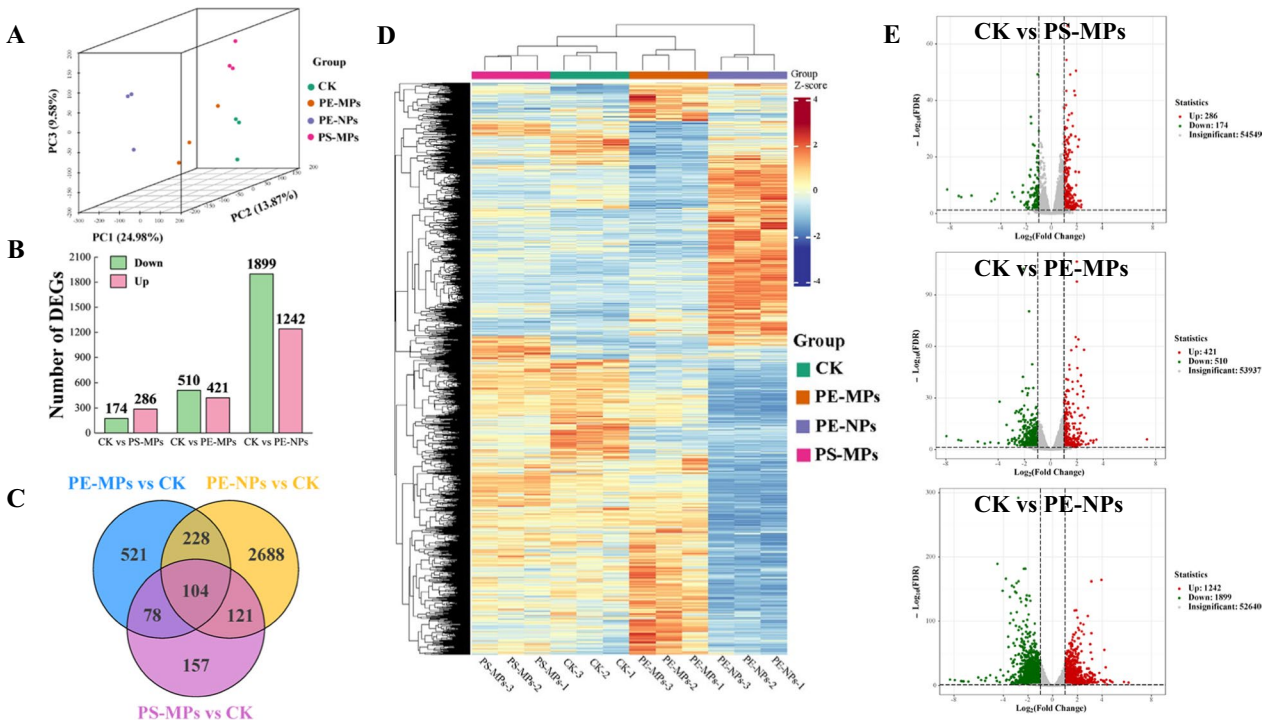

Fig. 6 The distribution of differentially expressed genes related to the responses of wheat in leaves after 30 days of N/MPs exposure. **A** 3D PCA of DEGs. **B** The regulation of DEGs, both up and down. **C** Pairwise compare the DEGs in groups on the Venn diagram. **D** Heatmaps of DEGs compared between different groups. **E** Volcano plots displaying the genes that are up- and down-regulated. Red plots represent upregulated genes; green plots represent downregulated genes; gray plots represent genes with no significant difference

lowest q-value, consistent with the findings of the photosynthetic parameters (Fig S2A). KEGG pathway analysis revealed that all N/MPs treatments highly affected the 'Metabolic Pathways', 'Biosynthesis of Secondary Metabolites', 'Plant Pathogen Interaction', and 'MAPK (Mitogen-Activated Protein Kinase) Signaling Pathway-Plant'. Plant hormone signal transduction showed high enrichment in PE-MPs and PE-NPs. Bubble chart results showed there was no significant differential enrichment of the KEGG pathway in PS-MPs. The KEGG pathway analysis of PE-MPs revealed significant enrichment in pathways including 'Carbon Fixation in Photosynthetic Organisms', 'Protein Processing in Endoplasmic Reticulum', 'Glyoxylate and Dicarboxylate Metabolism', 'Spliceosome', 'Carbon Metabolism', and 'Photosynthesis' (Padj < 0.05). The KEGG pathways of DEGs in PE-NPs were significantly enriched in 'Biosynthesis of Secondary Metabolites', 'Metabolic Pathways', 'Circadian Rhythm-plant', 'Benzoxazinoid Biosynthesis', 'Glycerophospholipid Metabolism', 'Carotenoid Biosynthesis', 'MAPK Signaling Pathway-plant', 'Monoterpenoid Biosynthesis', 'Steroid Biosynthesis', 'Photosynthesis-antenna Proteins', 'Plant-pathogen Interaction', 'Exopolysaccharide Biosynthesis', and 'Photosynthesis'. Wheat plants exposed to PE-MPs primarily stimulated plant development by controlling the metabolism of carbon, organic acids, and proteins. However, to maintain bioactivity and counteract the toxicity of PE-NPs, the biological activity of plants exposed to these particles mostly depended on 'Photosynthesis', 'Carbohydrate Metabolism', and 'Biosynthesis of Secondary Metabolites and Defensive Compounds' (Fig S2B).

Joint transcriptome and metabolomic analysis of N/MPs treatment in wheat

Integrating metabolomics and transcriptomics results, we conducted further joint analysis on the photosynthetic pathway, differential metabolomic pathways, MAPK, and PST (Plant-Signaling Transduction) signal cascades (Fig. 7). Under exposure to PE-NPs (Fig. 7A), several key genes related to Photosystem II (Psb A, Psb B, Psb C, Psb H, Psb P, Psb R, and Psb 28), Photosystem I (Psa A and Psa B), Cytochrome b6/f complex (PetA), Photosynthetic electron transport (PetF), F-type ATPase (beta and a), and ATP phosphohydrolase showed significant down-regulation ($p < 0.05$). In contrast, most of these genes exhibited significant up-regulation in PS-MPs treatment ($p < 0.05$) (Fig. 7A).

Additionally, the 'Flavonoid Biosynthesis', 'Carbon and Nitrogen Metabolism', and 'Plant Hormone Signal Transduction' pathways were affected by N/MPs exposure (Fig. 7B). PE-NPs treatment led to a notable accumulation of sucrose and D-Fructose-6P in the starch and sucrose metabolism pathway, while PS-MPs and PE-MPs treatments did not yield similar results. Moreover, treatment with PE-NPs markedly raised the expression of the HK and GPI genes while decreasing the beta-amylase gene. Tyrosine, phenylalanine, tryptophan, L-lysine, L-glutamate, L-leucine, L-isoleucine, L-arginine, and proline significantly accumulated after receiving PE-NPs and PS-MPs treatments. Gene expression of GLUD1_2, NirA, Nrt, NR, and TAT was significantly downregulated. Flavonoids, including cinnamic acid, caffeoyl quinic acid, caffeic acid, naringenin, eriodictyol, and myricetin, demonstrated a noteworthy increase in content specifically in response to PE-NPs treatment. The gene expression of CYP98A and CYP75B1 was significantly downregulated exclusively following PE-NPs treatment. Under PS-MPs and PE-NPs treatments, the relative abundance of HCT genes decreased, whereas CHS and FLS genes exhibited an increase (Fig. 7B).

In the context of MAPK and PST signal cascades (Fig. 7C), the contents of salicylic acid and jasmonic acid displayed opposing trends for all treatments. Particularly, in the exposure to PE-NPs, the content of salicylic acid was the highest and jasmonic acid was the lowest, being 3.04 and 0.15 times higher or lower than that of CK, respectively. Brassinosteroid was down-regulated with treatment of PE-NPs and up-regulated with treatment of PE-MPs. Furthermore, PE-NPs significantly down-regulated PP2C genes while up-regulating genes implicated in phytohormone signaling pathways, including NPR1, JAZ, BAI1, BSK, BZR1/2, and 734A1. The MAPK signaling pathway's involved genes, including WRKY22/29, MKK4/5, and MEKK1, were also significantly up-regulated in the PE-NPs group.

Rhizosphere bacterial responses to N/MPs stress

After PE-NPs treatment, there was a significant increase in rhizosphere bacterial species richness (Fig. 8A), while the greatest change in microbial species diversity was observed after PS-MPs treatment (Table. S2). Variations in the number of operational taxonomic units (OTUs) for various treatments were depicted in the Venn diagram analysis (Fig. 8B), with PE-NPs having the most OTUs (2555) and CK the fewest (2281). Common OTUs numbered 628 across the four treatments, while distinct OTUs were 980 (CK), 1149 (PE-MPs), 1101 (PS-MPs), and 1175 (PE-NPs). *Proteobacteria* (40.4–48.1%) and *Actinobacteriota* (25.6%–31.2%) were the major phyla (Fig. 8C), showing notable variations between treatments (Fig. 8D). *Proteobacteria* increased significantly with PE-NPs treatment, while *Actinobacteriota* and *Acidobacteriota* decreased. Conversely, *Actinobacteriota* and *Acidobacteriota* increased with PE-MPs and PS-MPs, respectively, while *Proteobacteria* decreased. The relative abundances of the top 20 genera are depicted in Fig. 8E,

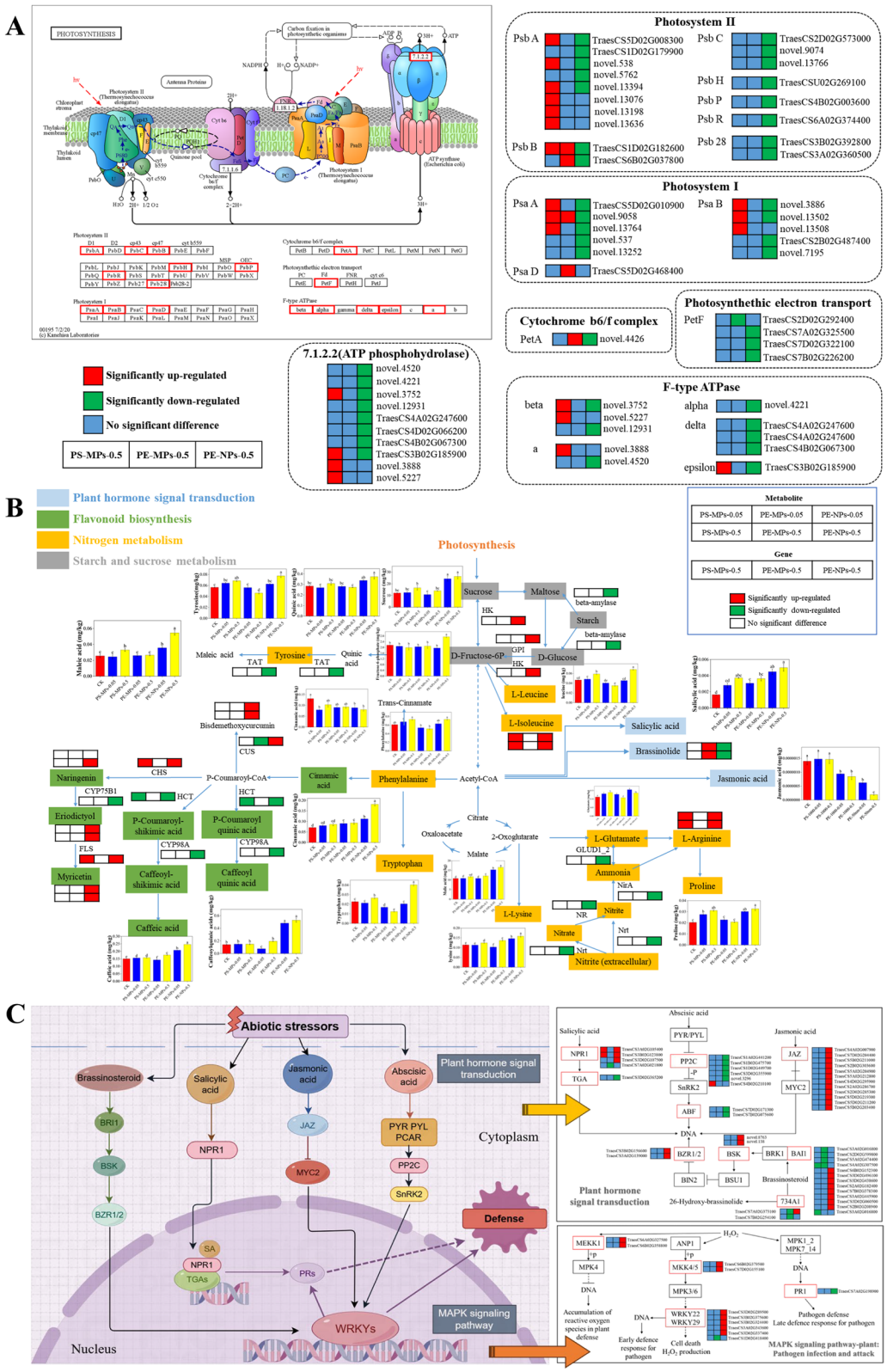

Fig. 7 The effects of N/MPs on photosynthesis, metabolic, and signal transduction pathways in wheat leaves: **A** photosynthesis, **B** Changes in pathways such as carbon and nitrogen metabolism after N/MPs treatment (The bar chart displayed the content of specific metabolites (mg/kg)), **C** The changes in MAPK and PST signal cascades in response to N/MPs treatment

with *Sphingomonas*, *Lysobacter*, *Massilia*, *Sphingomonadaceae*, *Micrococcaceae*, and *Nocardioides* being dominant. Compared to CK, PE-MPs treatment decreased the relative abundance of all major bacterial species (Fig. 8F). *Massilia* and *Lysobacter* significantly increased in the PE-NPs group, while other dominant genera decreased. Under PS-MPs treatment, most dominant genera decreased except for *Lysobacter* and *Nocardioides*.

At the phylum level, *Bacteroidota* and *Proteobacteria* exhibited greater abundance after PE-NPs treatment, while *Actinobacteriota*, *Acidobacteriota*, and *Chloroflexi* were significantly abundant in the PS-MPs group, according to the results of the linear discriminant analysis effect size (LEfSe) (Fig. 8G). In the rhizosphere soil of the CK, PE-MPs, and PE-NPs groups, only one clade displayed significant abundance at the genus level in each group. These findings corroborate our previous observations. Exposure to PE-NPs and PE-MPs upregulated all level-2 metabolic pathways, genetic information processing, environmental information processing, and cellular activities. In contrast, exposure to PS-MPs downregulated these functions. Regarding organismal systems, PE-NPs, PE-MPs, and PS-MPs all downgraded the immune system and excretory system, while only PE-NPs upgraded the environmental adaptation, endocrine system, and digestive system (Fig. 8H).

The relationship between rhizosphere soil bacteria and wheat photosynthesis

PICRUST2 was utilized to predict the relative abundances of genes involved in the cycling of phosphorus, sulfur, and nitrogen (Fig. 9A–C). After the N/MP treatments, there was a notable rise in the nitrogen cycle within the PS-MPs group, while a considerable decline was observed in the PE-NPs groups concerning genes associated with nitrification (amoA/B/C and hao genes), assimilatory nitrate reduction (nirA gene), and dissimilatory nitrate reduction (nrfA gene) ($p < 0.05$). In the nitrogen cycle, plants absorb nitrogen elements from the soil through their roots, converting them into organic substances such as proteins and nucleic acids. PS-MPs may enhance wheat plant photosynthesis by boosting the activities of photosynthetic nitrogen-metabolizing enzymes in rhizosphere bacteria, thereby promoting

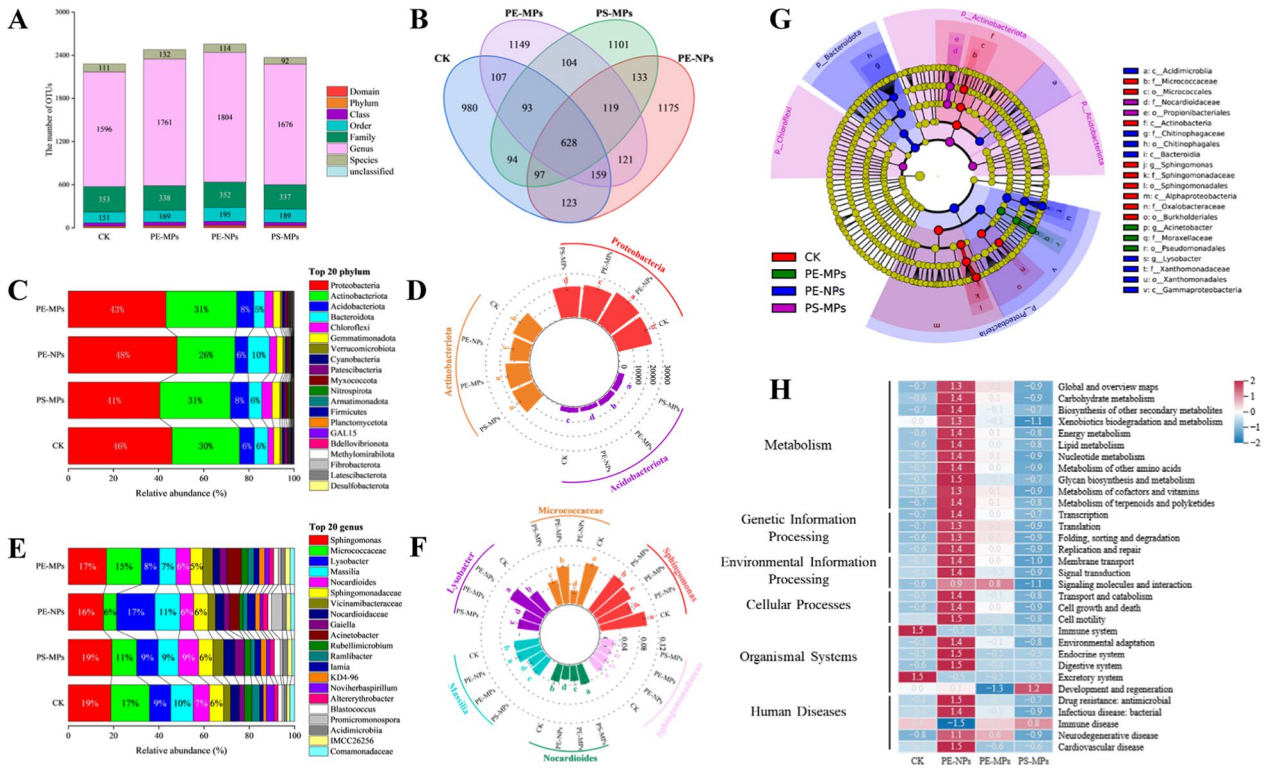

Fig. 8 Effects of N/MPs on the rhizosphere bacterial community. **A** The richness of the bacterial community at OTU levels. **B** Venn diagram of bacterial communities at OTU levels. **C** Relative abundance of bacteria community composition components at the phylum level (top 20). **D** The differential bacteria at the phylum level. **E** Relative abundance of bacteria community composition components at the genus level (top 20). **F** The differential bacteria at the genus level. **G** Cladogram of LEfSe results (from phylum to genus level) according to the different groups. **H** Functional categories of the bacterial communities estimated by PICRUSt2 at KEGG level 2

nitrogen absorption and assimilation. Conversely, PE-NPs elevated the expression of denitrification-related genes (nosZ, norB, and nirK). Denitrification is a significant contributor to nitrogen loss in soil, disrupting the natural nitrogen cycling process and impeding plant nitrogen uptake, consequently inhibiting photosynthesis [22].

Concerning the phosphate cycle, N/MPs had a primary impact on inorganic phosphorus solubilization and organic phosphorus mineralization compared to the CK. Within the PE-NPs treatment group, there was a significant increase in the relative abundance of appA, gcd, glpQ, and phoA genes, alongside a significant decrease in the ppa gene. The PS-MPs group demonstrated significantly elevated levels of ppx and glpQ. Conversely, the PE-MPs group exhibited substantially higher relative abundance levels of ppa and glpQ genes (Fig. 9B).

In the sulfur cycle, the relative abundance of genes associated with assimilatory sulfate reduction (cysC, cysH, and cysN/D/sat) was significantly reduced. Meanwhile, the PE-NPs treatment substantially enhanced the expression of aprA/B and dsrA/B genes associated with dissimilatory sulfate reduction. Conversely, following PS-MPs treatment, there was an increase in the relative abundances of cscC, cscJ/I, and cysH genes (Fig. 9C).

Figure 9D presents the heatmap resulting from correlation analysis between photosynthetic parameters and the rhizosphere soil microbial community. At the phylum level, *Proteobacteria*, *Deferribacterota*, *Fibrobacterota*, *Bacteroidota*, *Hydrogenedentes*, *Campylobacterota*, *DTB120*, *Gemmatimonadota*, *Bdellovibrionota*, *Myxococcota*, *Armatimonadota*, *Acidobacteriota*, *Actinobacteria*, and *Cyanobacteria* exhibited significant associations with wheat photosynthesis ($P < 0.05$). Among these, the most strongly correlated phyla were primarily *Proteobacteria*, *Deferribacterota*, *Bdellovibrionota*, *Myxococcota*, *Armatimonadota*, and *Cyanobacteria* (with more than 5 significant correlations). The first two exhibited negative correlations, while the last four showed positive correlations.

In the photorespiratory pathway, *Lysobacter* and *Massilia* from the *Proteobacteria* phylum, *Niastella* from the *Bacteroidota* phylum, and *Nocardioides* and *Promicromonospora* from the *Actinobacteriota* phylum exhibited the highest connectivity levels, as indicated by Weighted Gene Co-Expression Network Analysis (WGCNA). Regarding the sucrose biosynthesis pathway, *Flavitalea* from the *Bacteroidota* phylum, *unclassified_Sphingomonadaceae* from the *Proteobacteria* phylum, *Lechevalieria* from the *Actinobacteriota*

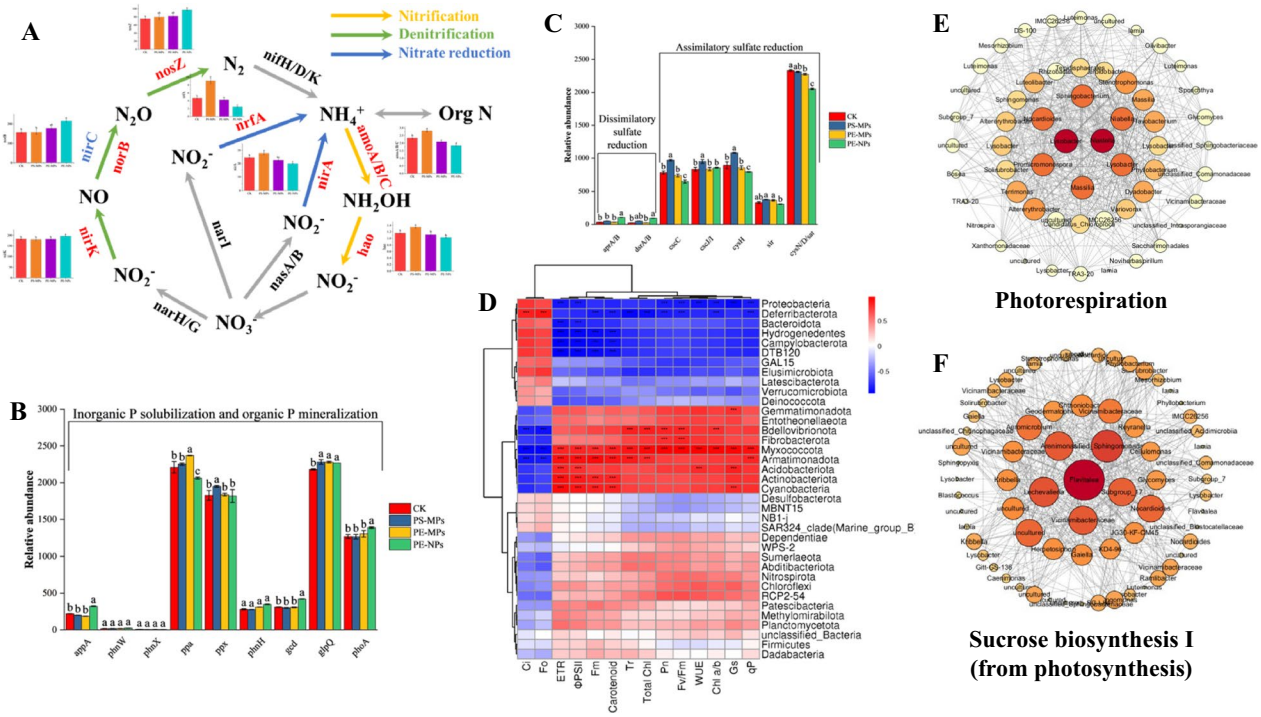

Fig. 9 Relative changes of nitrogen- (**A**), phosphorous- (**B**), and sulfur- (**C**) cycling genes in rhizosphere bacteria. The genes that showed significant abundance differences are red highlighted and their corresponding normalized abundances are displayed as bar plots; (**D**) Cluster heatmap of correlation between bacterial phyla and photosynthetic parameters; Rhizosphere bacteria genus co-expression networks: (**E**) Photorespiration, and (**F**) sucrose biosynthesis

phylum, *Vicinamibacteraceae* from the *Acidobacteriota* phylum, and *Arenimonas* from the *Proteobacteria* phylum demonstrated the highest connectivity levels.

N/MPs in soil-wheat system: Impact profile

We employed PLSPM analysis to elucidate the relationships among wheat biomass, photosynthesis, metabolites, genes, antioxidant activity, and microbial diversity, aiming to illustrate the impact of various N/MPs treatments on the wheat-soil system Fig. 10). The PLSPM analysis revealed that the type of N/MPs had a positive direct effect on genes (0.2311), metabolites (0.6644), and microbial diversity (0.0141), while negatively impacting wheat biomass (− 0.6248), photosynthesis (− 0.6067), and the antioxidant system (− 0.5473). The size of N/MPs had a positive direct effect on genes (1.4988) and metabolites (1.3697), but a negative direct effect on wheat biomass (− 0.7259), photosynthesis (− 0.3753), microbial diversity (− 1.7961), and the antioxidant system (− 1.0701). Except for photosynthesis, the size of N/MPs had a greater impact on other parameters, whereas the type of N/MPs had a more pronounced effect on photosynthesis. Wheat photosynthesis was significantly positively influenced by microbial diversity (0.7173), and in turn, photosynthesis had a positive impact on plant growth (0.9871). These findings indicate that soil microorganisms play a crucial role in regulating plant biomass by influencing photosynthesis. Furthermore, PE-MPs and PE-NPs exhibited a more pronounced adverse effect compared to PS-MPs (Fig. 10C–E). This was evidenced by total effect values of 0.7889, 0.9983, 0.9720, and 0.0032 in the PS-MPs treatment on wheat biomass, photosynthesis, rhizosphere bacteria, and the antioxidant system, while the values were − 0.0663, − 0.0653, − 0.18432, and 0.31 for the PE-MPs, and − 0.964, − 0.998, − 0.968, and − 0.5032 for the PE-NPs treatments, respectively. The PLSPM results strongly supported the interpretation of the multi-omics data.

Discussion

At high concentrations, PE-NPs inhibited photosynthesis and disrupted the normal growth of wheat plants, as indicated by wheat phenotypic and photosynthetic parameters. The observed reduction in PSII reaction center openness in the PE-NPs treatment may hinder the rate of electron transfer during photosynthetic respiration, leading to photoinhibition [23]. The downregulation of PsaA, a key protein in the transmembrane complex of photosystem I which is essential for NADPH synthesis [24], adversely affects the synthesis rate of proteins in photosystem I reaction center and NADPH synthesis. Another indication of inhibited electron transfer and

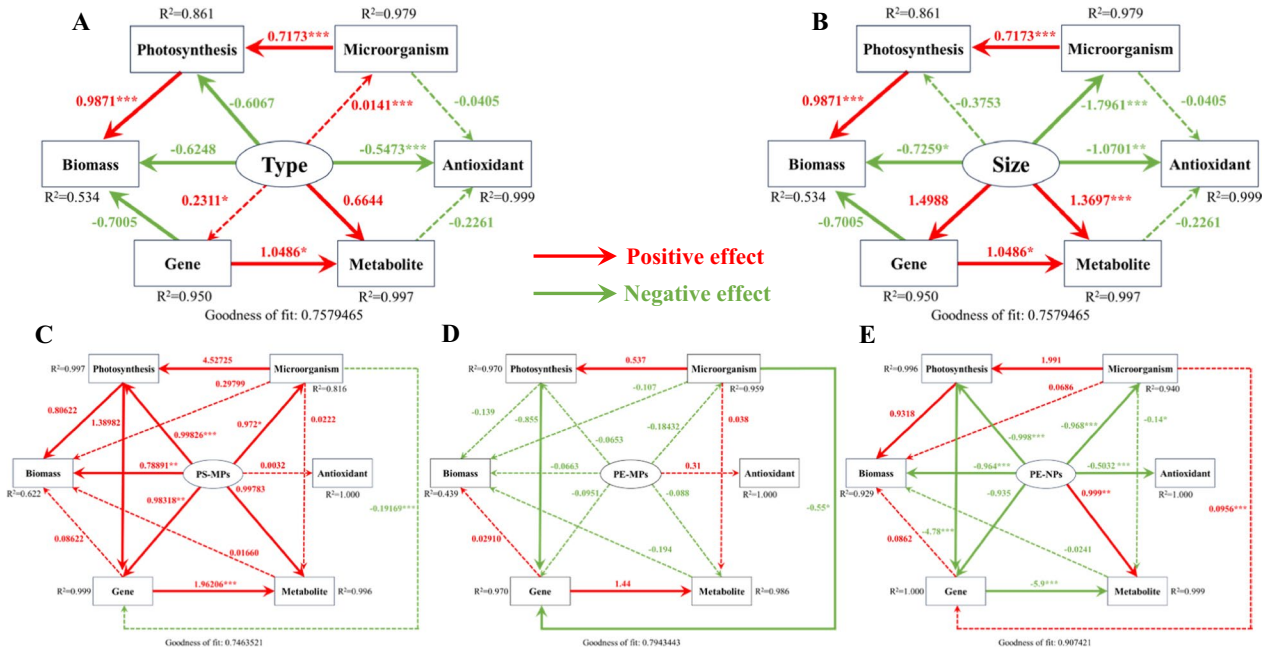

Fig. 10 The PLSPM for data from the type (**A**), size (**B**), PS-MPs (**C**), PE-MPs (**D**), and PE-NPs (**E**) treatments. Each rectangle represents a latent variable indicated by a set of manifest variables. The arrow widths are proportional to the strength of the path coefficient, with only significant paths marked with a star (*, **, and *** representing significance levels of $p < 0.05$, $p < 0.01$, and $p < 0.001$, respectively). Red arrows indicate positive effects between latent variables, while green arrows indicate negative effects. R^2 represents the proportion of variance explained. The goodness of fit values > 0.7 represents a good prediction for the entire model

reduced NADPH synthesis, which affects ATP synthesis and overall photosynthetic capability, is the downregulation of Fd, the final electron acceptor in photosystem I [25]. These downregulations may result from the oxidative stress induced by PE-NPs, which disrupted cellular redox balance and damaged the cellular components of wheat plants. Both Fd (ferredoxin) and PsaA (a core protein of PSI) are crucial components of PSI, and oxidative stress may inhibit the expression of these genes by damaging these proteins or by affecting the signaling pathways that regulate their expression [26]. Another possible reason is that PE-NPs inhibited the nitrification and nitrate reduction in rhizosphere bacteria, thus promoted denitrification and reduced nitrogen uptake by plants. Consequently, plants respond to nutrient deficiency by downregulating Fd and PsaA gene expression to adapt to low-nutrient environments. The observed reduction in plant biomass under PE-NPs stress corresponds with the negative effects on photosynthesis.

Compared to PS-MPs at equivalent concentrations and sizes, PE-MPs treatment increased the activities of antioxidant enzymes SOD, POD, and CAT, indicating a stronger oxidative stress response in wheat. This may be caused by several factors: Firstly, the chemical structure and properties of PE and PS differ, leading to varied interactions within plant cells. PE is non-polar and highly hydrophobic, and may interact differently with cellular components compared to the slightly polar PS [27]. Additionally, the surface chemistry and reactivity of PE might disrupt cell membrane integrity more than PS, inducing stronger oxidative stress responses [28]. PE is also likely to generate higher levels of ROS within plant cells, exacerbating oxidative damage. These combined factors contribute to the more severe oxidative stress observed in wheat plants that exposed to PE-MPs compared to PS-MPs. Notably, when particle sizes were reduced to 50 nm, wheat plants struggled to maintain redox homeostasis, leading to the accumulation of harmful substances such as MDA. Plants maintain free radical homeostasis through enzymatic antioxidant systems. SOD, POD, and CAT are essential for scavenging reactive oxygen species (ROS) produced during abiotic stressors. SOD catalyzes the conversion of $O_2^{\bullet -}$ to H_2O_2, a less toxic compound, which is then eliminated by CAT and POD [29]. In this study, PS-MPs and low concentrations of PE-MPs did not have a significant impact on the antioxidant system of wheat. Higher concentrations of PE-MPs and lower concentrations of PE-NPs enhanced antioxidant enzyme activities, thus preventing oxidative stress damage. However, under severe stress, the activities of SOD, POD, and CAT were significantly reduced at concentration of 0.5 g/kg of PE-NPs. This led to a substantial generation and accumulation of MDA, causing damage to the cell membrane.

Amino acids play diverse and crucial roles in plants, serving as the fundamental building blocks of proteins. Additionally, they are involved in various biochemical processes, including photosynthesis, nitrogen metabolism, and stress tolerance [30]. The presence of PE-NPs disrupted the metabolic levels of several amino acids, such as phenylalanine, tryptophan, L-lysine, L-glutamate, L-leucine, L-isoleucine, L-arginine, and proline. This disruption suggests significant perturbations in key metabolic pathways, including 'Glutathione Metabolism,' 'Alanine, Aspartate, and Glucose Metabolism,' and 'Arginine Biosynthesis' (Fig. 7B), which are indicative of broader disruptions in nitrogen metabolism in wheat. Under stress conditions, the biosynthesis of proline is often accelerated. Proline serves multiple protective functions: it acts as an osmoprotectant, stabilizing subcellular structures and scavenging free radicals, and also helps in consuming excess NADPH, thereby reducing ROS generation [31]. The significant increase in substances like malic acid after PE-NPs treatment further supports this observation. Malic acid acts as an osmoregulatory substance, and it is crucial for protecting cellular membranes from damage and mitigating osmotic pressure imbalances caused by abiotic stresses, thereby enhancing plant tolerance to adverse conditions [32]. Phenylalanine and tryptophan are essential for synthesizing antioxidants, such as flavonoids, which play a pivotal role in combating oxidative stress. These antioxidants help neutralize ROS, thereby protecting the plant cells from oxidative damage. Additionally, L-glutamate, L-leucine, L-isoleucine, and L-arginine are closely associated with plant resistance mechanisms, since they participate in the synthesis of stress- responsive proteins that enhance the plant's tolerance to adverse conditions [33]. The observed changes suggested that the amino acid metabolic systems were activated in the wheat plants to produce necessary amino acids and other protective substances in response to the stress induced by PE-NPs. This activation supports various physiological processes essential for maintaining cellular homeostasis and mitigating stress impacts. Consequently, the modulation of amino acid metabolism appears to be a crucial adaptive mechanism enabling wheat to cope with nanoparticle-induced stress (Fig. 7B).

Exposure to PE-NPs triggered the pathway of 'Stilbenoid, Diarylheptanoid, and Gingerol Biosynthesis', resulting in a notable up-regulation of genes associated with the CYP98A and CUS enzymes. This activation led to the accumulation of antioxidants such as bisdemethoxycurcumin and chlorogenic acid (Fig. 7B). The key players in the defense against abiotic stressors are CYP98A and CUS enzymes. CYP98A is a cytochrome P450 enzyme, which catalyzes the conversion of 5-O-p-Coumaroyl-CoA to chlorogenic acid, and is known for its antioxidant

properties. Chlorogenic acid plays a significant role in absorbing excess ROS and reducing membrane lipid peroxidation, thereby protecting cells from oxidative damage. The CUS enzyme (curcumin synthase) promotes the conversion of P-Coumaroyl-CoA to Bisdemethoxycurcumin, which is also a potent antioxidant [34]. The up-regulation of CYP98A and CUS in response to PE-NP exposure indicated an adaptive mechanism in wheat plants, by which the antioxidant defense systems were enhanced to mitigate the oxidative stresses. In particularly, chlorogenic acid is effective in neutralizing ROS, which are highly reactive molecules that can cause significant damage to cellular components, such as lipids, proteins, and nucleic acids. By decreasing membrane peroxidation, chlorogenic acid helps maintain cell membrane integrity and cell function under stress conditions [35]. Bisdemethoxycurcumin also contributes to the antioxidant defense, further supporting the plant's ability to counteract the oxidative stress induced by PE-NPs.

Flavonoids, with their diverse structures, are effective in scavenging ROS, thereby protecting cellular components from oxidative damage and maintaining redox homeostasis [36]. Under exposure to PE-NPs, the up-regulation of the flavonoid biosynthesis pathway likely served as a crucial adaptive response. Flavonoids not only act as direct antioxidants but also modulate other defense-related pathways, enhancing the plant's overall resilience to stress. For instance, flavonoids can chelate metal ions and inhibit lipid peroxidation, thereby protecting membrane integrity and function under stress conditions [37]. Furthermore, the synthesis of flavonoids involves key enzymes such as chalcone synthase (CHS), which were up-regulated under stress conditions (Fig. 7B). These enzymes facilitate the conversion of primary metabolites into flavonoid precursors, leading to an accumulation of flavonoids that fortify the plant's antioxidant defense system. The increased production of flavonoids, while beneficial for stress tolerance, indicates a trade-off where growth and biomass accumulation might be compromised due to the diversion of resources towards secondary metabolite production. This resource allocation highlights the complex balance between defense mechanisms and growth processes, underscoring the plant's strategic prioritization of immediate survival over growth under adverse conditions induced by PE-NPs.

The interaction between WRKY transcription factors (WRKY TFs) and various signaling pathways highlights the complexity of plant stress responses and adaptation mechanisms. PE-NPs can induce oxidative stress in plants, which subsequently triggers the activation of MAPK signaling pathways. This pathway comprises a cascade of protein kinases, including MEKK1 and MKK4/5, which phosphorylate and activate WRKY TFs such as WRKY22/29. The activation of these TFs leads to the transcription of stress-responsive genes that help in mitigating the effects of both biotic and abiotic stressors [38]. WRKY TFs also exhibit cross-talk with hormone signaling pathways, integrating environmental signals to fine-tune the plant's response. For instance, WRKY22/29 can modulate the salicylic Acid (SA) signaling pathway through interaction with NPR1, a key regulator of SA-mediated defense responses. Similarly, they influence the JA signaling pathway by interacting with ZIM domain (JAZ) proteins, which are repressors of jasmonic acid (JA) signaling and are involved in defense and developmental processes. The brassinosteroid (BR) signaling pathway, mediated by brassinosteroid insensitive 1 (BAI1), and the ABA signaling pathway, involving protein phosphatase 2C (PPWC) and ABA responsive element binding factor (ABF), are also regulated by WRKY TFs. These interactions collectively regulate the expression of genes involved in nutrient absorption and growth hormone biosynthesis, which are crucial for plant adaptation and survival under stress conditions induced by PE-NPs. In summary, the interplay between MAPK signaling, WRKY TFs, and hormone pathways under PE-NPs stress involves a multi-faceted regulatory network. This network integrates various signals to optimize plant growth and stress resistance, highlighting the complex mechanisms by which plants respond to environmental challenges. [39–41].

Analysis of the Chao, Shannon, and Simpson indices revealed that exposure to PE-NPs increased the α-diversity of the bacteria community (Table S2). The increase in diversity suggests a positive response of the microbial community to PE-NPs exposure, potentially indicating an adaptive mechanism or niche diversification. *Proteobacteria* and *Bacteroidota* exhibited a higher relative abundance after treatment with PE-NPs, suggesting that some bacterial phyla may have the ability to degrade NPs or resist NP-induced stress. At the genus level, notable observations include the dominance of genera belonging to the *Proteobacteria* phylum across all groups (Fig. 8E). This phylum is known for its diverse metabolic capabilities and environmental adaptability. PE-NPs notably increased the abundance of *Lysobacter*, a member of the *Proteobacteria* phylum with documented capabilities in plastic and additive degradation [42]. *Lysobacter* species produce various extracellular enzymes and secondary metabolites that can break down complex polymers, making them effective in degrading polyethylene and other synthetic materials. The increase of *Lysobacter* suggests that *Lysobacter* might play a crucial role in the microbial degradation of PE-NPs in the rhizosphere soil.

Furthermore, PE-NPs and PS-MPs facilitated the formation of aerobic genera such as *Nocardioides* and *Massilia* (Fig. 8F). These genera have been reported to utilize nanoparticles and microplastics as carbon sources, enhancing their degradation. *Nocardioides* species are known for their ability to degrade a wide range of organic pollutants, including plastics, through oxidative and hydrolytic enzymatic pathways. Similarly, *Massilia* species are versatile in utilizing various carbon sources, including synthetic polymers, suggesting their potential role in microplastic degradation in soil environments [43, 44].

In addition to the observed taxonomic differences, the bacterial communities in the various N/MPs treatment groups exhibited distinct functional compositions and patterns of gene abundance associated with the cycling of nitrogen, phosphorus, and sulfur. These changes were influenced by the characteristics of N/MPs, which play critical roles in soil nutrient cycling and plant growth. Soil microorganisms are essential for enhancing biomass and plant growth due to their roles in sulfur metabolism, nitrogen fixation, and phosphorus solubilization [45]. After PE-NPs treatment, microbial nitrogen cycles exhibited notable differences, with enriched denitrification processes and decreased dissimilatory and assimilatory nitrate reduction in the rhizosphere. Denitrification is a process leads to the conversion of nitrate to nitrogen, which results in nitrogen loss from the soil, and consequently reducing the nitrogen availability for plant uptake. The reduction in available nitrogen can negatively impact plant photosynthesis and growth, as nitrate is a crucial nitrogen source for plants. Transcriptome data revealed that PE-NPs significantly decreased the expression of nitrate transporter (Nrt) and nitrate reductase (NR) genes. Nrt is responsible for transporting nitrate and nitrite from extracellular regions into the intracellular space, while NR aids in converting nitrate to nitrite. Following this conversion, nitrite is transformed to ammonium nitrogen by nitrite reductase (NiR), and glutamine synthetase/glutamate synthetase (GS/GOGAT) then produces organic nitrogen molecules such as glutamic acid. These organic nitrogen molecules are vital for the synthesis of amino acids and other organic substances [46]. By interfering with the nitrogen cycle, PE-NPs likely decreased the efficiency of nitrogen utilization in wheat leaves, resulting in reduced nitrogen transport and nitrate production catalyzed by NR. This disruption in nitrogen metabolism can lead to decreased chlorophyll concentration and net photosynthetic rate, ultimately affecting plant growth. PE-NPs also impacted the sulfur cycle in the soil by decreasing the abundance of genes associated with the assimilatory sulfate reduction and by increasing those genes involved in dissimilatory sulfate reduction. In the process of dissimilatory sulfate reduction, soil sulphate is converted to sulphide, which is less readily available for plant uptake. Sulfur is an essential element for plants, and the decrease in its availability can negatively impact plant growth and development [47]. Additionally, dissimilatory sulfate reduction releases hydrogen sulfide ions, which can lead to the acidification of soil, further complicating the nutrient uptake of wheat plants [48]. Conversely, PS-MPs promoted nitrification and nitrate reduction processes in the rhizosphere bacterial nitrogen cycle, as well as the assimilatory sulfate reduction processes in the sulfur cycle. Nitrification and nitrate reduction processes enhance the availability of nitrate, a crucial nitrogen source for plants, thereby supporting plant growth and photosynthesis. Similarly, assimilatory sulfate reduction converts sulfate to organic sulfur that can be readily uptake by plants, therefore promoted the acquisition of essential sulfur for plants. These processes are beneficial for plant nutrient uptake and overall health, facilitating better photosynthetic performance and growth.

The plant body is a complex integrated system where the growth of the aboveground part is closely linked to the root system and soil microorganisms. According to this study, the type, size, and dosage of N/MPs in soil significantly influenced the photosynthesis, metabolites, antioxidant system, and rhizosphere soil bacterial community of wheat plants. Among them, PE-NPs were found to have the most adverse effects on wheat growth and development. The correlation analysis revealed that microbial diversity had a significant positive impact on wheat photosynthesis. Enhanced microbial diversity could support various beneficial microbial activities, such as nutrient cycling and stress tolerance, which collectively promote healthier and more efficient photosynthesis. This improved photosynthesis had a strong positive impact on plant growth, indicating that soil microorganisms played a crucial role in determining plant biomass by influencing photosynthesis.

Conclusion

This study intensively investigated the effects of NPs and MPs of PE and PS on the growth and stress response of wheat, as well as the rhizosphere microbial community using metabolomics and transcriptomics approaches. PS and PE exhibited different effects at different particle size and concentration.PE-NPs dramatically inhibited soil bacterial diversity and interfered with the expression of functional genes related to nitrogen and sulfur cycling in rhizosphere bacteria, thereby preventing plants from absorbing essential elements from the soil and inhibiting wheat photosynthesis and growth. Wheat plants responded to the stress of PE-NPs by modulating metabolites and gene expression in key pathways

like flavonoid biosynthesis, nitrogen metabolism, and MAPK signaling, aiming to recalibrate biochemical processes and prioritize survival. Significant disruptions in nitrogen metabolism and increased flavonoid content in the wheat leaves indicated a strategic shift to cope with the oxidative stress from the NPs. Under PE-NPs stress, WRKY transcription factors interact with MAPK, SA, JA, BR, and ABA signaling pathways to regulate nutrient absorption and growth hormone biosynthesis, ultimately enhancing plant stress resistance and adaptation. Compared with PE-NPs, the negative impact of PE-MPs on the wheat-soil system was relatively small. However, the effects of PS-MPs appeared to be opposite in terms of photosynthesis, plant metabolism, and functional gene expression in soil rhizosphere bacterial communities. Further research is needed to explore the roles of different MP properties in plant toxicology. The results preliminarily elucidate the molecular mechanisms of wheat's response to nano- and microplastic stress, laying a theoretical foundation for future studies on plant adaptation and resistance to environmental pollutants. This could also guide the development of crop improvement strategies in agricultural practices to mitigate pollution stress.

Supplementary Information

The online version contains supplementary material available at https://doi.org/10.1186/s12951-024-02777-x.

Supplementary Material 1.

Acknowledgements
This work was supported by National key research and development program (2023YFD1400902); Beijing Natural Science Foundation (no. J210019); Hebei Natural Science Foundation (no. C2021204190); Tianjin Natural Science Foundation (no. 21JCZXJC00110).

Author contributions
MZ, CQ, YB, MC and SW for the Conceptualization, Data curation, Formal analysis, and writing the original draft. LG, RP and HX for the Investigation, Methodology. LH for the Funding acquisition, Project administration, and Supervision. All authors have read and approved the manuscript.

Availability of data and materials
All data generated or analyzed during this study are included in this published article within each editable graph. No datasets were generated or analysed during the current study.

Declarations

Ethics approval and consent to participate
Not applicable.

Consent for publication
Not applicable.

Competing interests
The authors declare that they have no known competing financial interests or personal relationships that could have appeared to influence the work reported in this paper.

Author details
[1]Innovation Center of Pesticide Research, Department of Applied Chemistry, College of Science, China Agricultural University, 2 Yuanmingyuan Western Road, Haidian District, Beijing 100193, China. [2]Zhengzhou Fruit Research Institute, Chinese Academy of Agricultural Sciences, Zhengzhou 450009, China. [3]Zhongyuan Research Center, Chinese Academy of Agricultural Sciences, Xinxiang 453514, China. [4]SCIEX Application Center, Shanghai 200233, China.

Received: 7 May 2024 Accepted: 14 August 2024
Published online: 23 August 2024

References

1. Bakaraki Turan N, Sari Erkan H, Onkal Engin G. Current status of studies on microplastics in the world's marine environments. J Clean Prod. 2021;327:129394. https://doi.org/10.1016/j.jclepro.2021.129394.
2. Zhang SY, He ZZ, Wu CY, Wang ZH, Mai YW, Hu RW, Zhang XJ, Huang W, Tian YH, Xia DH, Wang C, Yan QY, He ZL, Shu LF. Complex bilateral interactions determine the fate of polystyrenemicro- and nanoplastics and soil protists: implications from a soil amoeba. Environ Sci Technol. 2022;56:4936–49. https://doi.org/10.1021/acs.est.1c06178.
3. Maity S, Guchhait R, Sarkar MB, Pramanick K. Occurrence and distribution of micro/nanoplastics in soils and their phytotoxic effects: a review. Plant Cell Environ. 2022;45:1011–28. https://doi.org/10.1111/pce.14248.
4. Qiu XR, Ma SR, Zhang JX, Fang LC, Zhu LY, Guo XT. dissolved organic matter promotes the aging process of polystyrene microplastics under dark and ultraviolet light conditions: the crucial role of reactive oxygen species. Environ Sci Technol. 2022;56:10149–60. https://doi.org/10.1021/acs.est.2c03309.
5. Gao M, Chang J, Wang Z, Zhang H, Wang T. Advances in transport and toxicity of nanoparticles in plants. J Nanobiotechnology. 2023;21:75. https://doi.org/10.1186/s12951-023-01830-5.
6. Ali I, Cheng Q, Ding T, Yiguang Q, Yuechao Z, Sun H, Peng C, Naz I, Li J, Liu J. Micro- and nanoplastics in the environment: occurrence, detection, characterization and toxicity—a critical review. J Clean Prod. 2021;313:127863. https://doi.org/10.1016/j.jclepro.2021.127863.
7. Zhang XY, Li Y, Ouyang D, Lei JJ, Tan QL, Xie LL, Li ZQ, Liu T, Xiao YM, Farooq TH, Wu XH, Chen L, Yan WD. Systematical review of interactions between microplastics and microorganisms in the soil environment. J Hazard Mater. 2021. https://doi.org/10.1016/j.jhazmat.2021.126288.
8. Qi YL, Ossowicki A, Yang XM, Lwanga EH, Dini-Andreote F, Geissen V, Garbeva P. Effects of plastic mulch film residues on wheat rhizosphere and soil properties. J Hazard Mater. 2020. https://doi.org/10.1016/j.jhazmat.2019.121711.
9. Wang FY, Zhang XQ, Zhang SQ, Zhang SW, Sun YH. Interactions of microplastics and cadmium on plant growth and arbuscular mycorrhizal fungal communities in an agricultural soil. Chemosphere. 2020. https://doi.org/10.1016/j.chemosphere.2020.126791.
10. Jiang M, Li SX, Li HW, Jian SL, Liu FL, Li XN. Reprogramming of microbial community in barley root endosphere and rhizosphere soil by polystyrene plastics with different particle sizes. Sci Total Environ. 2023. https://doi.org/10.1016/j.scitotenv.2023.161420.
11. Zarus GM, Muianga C, Hunter CM, Pappas RS. A review of data for quantifying human exposures to micro and nanoplastics and potential health risks. Sci Total Environ. 2021;756:144010. https://doi.org/10.1016/j.scitotenv.2020.144010.
12. Li T, Cao XF, Zhao R, Cui ZJ. Stress response to nanoplastics with different charges in *Brassica napus* L. during seed germination and seedling growth stages. Front Env Sci Eng. 2023. https://doi.org/10.1007/s11783-023-1643-y.
13. Lian JP, Liu WT, Sun YB, Men SZ, Wu JN, Zeb A, Yang TZ, Ma LQ, Zhou QX. Nanotoxicological effects and transcriptome mechanisms of wheat (*Triticum aestivum* L.) under stress of polystyrene nanoplastics. J Hazard Mater. 2022. https://doi.org/10.1016/j.jhazmat.2021.127241.
14. Chen GL, Li YZ, Liu SL, Junaid M, Wang J. Effects of micro(nano)plastics on higher plants and the rhizosphere environment. Sci Total Environ. 2022. https://doi.org/10.1016/j.scitotenv.2021.150841.
15. Hasan MM, Jho EH. Effect of different types and shapes of microplastics on the growth of lettuce. Chemosphere. 2023;339:139660. https://doi.org/10.1016/j.chemosphere.2023.139660.

16. FAO, The Date on the Word Production of Maize, Rice (Paddy) and Wheat in 2017, (2017)
17. USEPA, Nanotechnology White Paper-External Review Draft, (2007)
18. Dhevagi P, Sahasa RGK, Poornima R, Ramya A. Unveiling the effect of microplastics on agricultural crops—a review. Int J Phytoremediat. 2024;26:793–815. https://doi.org/10.1080/15226514.2023.2275152.
19. Li RJ, Tu C, Li LZ, Wang XY, Yang J, Feng YD, Zhu X, Fan QH, Luo YM. Visual tracking of label-free microplastics in wheat seedlings and their effects on crop growth and physiology. J Hazard Mater. 2023;456:131675. https://doi.org/10.1016/j.jhazmat.2023.131675.
20. Yang L, Zhang Y, Kang S, Wang Z, Wu C. Microplastics in soil: a review on methods, occurrence, sources, and potential risk. Sci Total Environ. 2021;780: 146546. https://doi.org/10.1016/j.scitotenv.2021.146546.
21. Xu LL, Li J, Liu SS, Qin TL, Luo H, Zhou XX, Li W. Studies on root growth, yield and resilience of winter wheat under waterlogging control in Huaibei Plain, China. J Plant Growth Regul. 2024. https://doi.org/10.1007/s00344-024-11336-5.
22. Jiang L, Liu S, Wang S, Sun L, Zhu G. Effect of tillage state of paddy soils with heavy metal pollution on the nosZ gene of N(2)O reductase. J Environ Sci. 2024;137:469–77. https://doi.org/10.1016/j.jes.2023.02.024.
23. Qiu ZY, Wang LH, Zhou Q. Effects of bisphenol A on growth, photosynthesis and chlorophyll fluorescence in above-ground organs of soybean seedlings. Chemosphere. 2013;90:1274–80. https://doi.org/10.1016/j.chemosPhere.2012.09.085.
24. Murray JW, Duncan J, Barber J. CP43-like chlorophyll binding proteins: structural and evolutionary implications. Trends Plant Sci. 2006;11:152–8. https://doi.org/10.1016/j.tplants.2006.01.007.
25. Kimata-Ariga Y, Chikuma Y, Saitoh T, Miyata M, Yanagihara Y, Yamane K, Hase T. NADP(H) allosterically regulates the interaction between ferredoxin and ferredoxin-NADP+ reductase. FEBS Open Bio. 2019;9:2126–36. https://doi.org/10.1002/2211-5463.12752.
26. Li J, Zheng XW, Liu XL, Zhang LL, Zhang S, Li YY, Zhang WZ, Li QH, Zhao YQ, Chen XF, Wang XR, Huang HH, Fan ZQ. Effect and mechanism of microplastics exposure against microalgae: photosynthesis and oxidative stress. Sci Total Environ. 2023. https://doi.org/10.1016/j.scitotenv.2023.167017.
27. Polechonska L, Rozman U, Sokolowska K, Kalciková G. The bioadhesion and effects of microplastics and natural particles on growth, cell viability, physiology, and elemental content of an aquatic macrophyte. Sci Total Environ. 2023. https://doi.org/10.1016/j.scitotenv.2023.166023.
28. Mao YF, Ai HN, Chen Y, Zhang ZY, Zeng P, Kang L, Li W, Gu WK, He Q, Li H. Phytoplankton response to polystyrene microplastics: perspective from an entire growth period. Chemosphere. 2018;208:59–68. https://doi.org/10.1016/j.chemosphere.2018.05.170.
29. Li JL, Hu J, Ma CX, Wang YQ, Wu C, Huang J, Xing BS. Uptake, translocation and physiological effects of magnetic iron oxide (γ-Fe2O3) nanoparticles in corn (*Zea mays* L.). Chemosphere. 2016;159:326–34. https://doi.org/10.1016/j.chemosphere.2016.05.083.
30. Zhou JL, Vadiveloo A, Chen DZ, Gao F. Regulation effects of indoleacetic acid on lipid production and nutrient removal of chlorella pyrenoidosa in seawater-containing wastewater. Water Res. 2024. https://doi.org/10.1016/j.watres.2023.120864.
31. Alvarez ME, Savouré A, Szabados L. Proline metabolism as regulatory hub. Trends Plant Sci. 2022;27:39–55. https://doi.org/10.1016/j.tplants.2021.07.009.
32. Tahjib-Ul-Arif M, Zahan MI, Karim MM, Imran S, Hunter CT, Islam MS, Mia MA, Hannan MA, Rhaman MS, Hossain MA, Brestic M, Skalicky M, Murata Y. Citric acid-mediated abiotic stress tolerance in plants. Int J Mol Sci. 2021. https://doi.org/10.3390/ijms22137235.
33. Asad MAU, Guan XY, Zhou LJ, Qian Z, Yan Z, Cheng FM. Involvement of plant signaling network and cell metabolic homeostasis in nitrogen deficiency-induced early leaf senescence. Plant Sci. 2023. https://doi.org/10.1016/j.plantsci.2023.111855.
34. Wang ZH, Wang WP, Wu WT, Wang HL, Zhang S, Ye C, Guo LW, Wei ZX, Huang HP, Liu YX, Zhu SS, Zhu YY, Wang Y, He XH. Integrated analysis of transcriptome, metabolome, and histochemistry reveals the response mechanisms of different ages *Panax notoginseng* to root-knot nematode infection. Front Plant Sci. 2023. https://doi.org/10.3389/fpls.2023.1258316.
35. Soviguidi DRJ, Pan R, Liu Y, Rao LP, Zhang WY, Yang XS. Chlorogenic acid metabolism: the evolution and roles in plant response to abiotic stress. Phyton-Int J Exp Bot. 2022;91:239–55. https://doi.org/10.3260/phyton.2022.018284.
36. Nakabayashi R, Saito K. Integrated metabolomics for abiotic stress responses in plants. Curr Opin Plant Biol. 2015;24:10–6. https://doi.org/10.1016/j.pbi.2015.01.003.
37. Shen N, Wang TF, Gan Q, Liu S, Wang L, Jin B. Plant flavonoids: classification, distribution, biosynthesis, and antioxidant activity. Food Chem. 2022. https://doi.org/10.1016/j.foodchem.2022.132531.
38. Yu J, Zhang X, Cao J, Bai H, Wang R, Wang C, Xu Z, Li C, Liu G. Genome-wide identification and characterization of WRKY transcription factors in *Betula platyphylla* Suk. and their responses to abiotic stresses. Int J Mol Sci. 2023. https://doi.org/10.3390/ijms241915000.
39. Mukherjee A, Gaurav AK, Singh S, Yadav S, Bhowmick S, Abeysinghe S, Verma JP. The bioactive potential of phytohormones: a review. Biotechnol Rep. 2022;35:e00748. https://doi.org/10.1016/j.btre.2022.e00748.
40. Bari R, Jones J. Role of plant hormones in plant defence responses. Plant Mol Biol. 2009;69:473–88. https://doi.org/10.1007/s11103-008-9435-0.
41. Saha B, Nayak J, Srivastava R, Samal S, Kumar D, Chanwala J, Dey N, Giri MK. Unraveling the involvement of WRKY TFs in regulating plant disease defense signaling. Planta. 2024. https://doi.org/10.1007/s00425-023-04269-y.
42. Lin JY, Liu HT, Li XY, Li XW. Influence of sludge treatment methods on behaviors of microplastics adsorbed cadmium and its driving factors. J Environ Manage. 2022. https://doi.org/10.1016/j.jenvman.2022.116113.
43. Suzuki M, Tachibana Y, Takizawa R, Morikawa T, Takeno H, Kasuya K. A novel poly(3-hydroxybutyrate)-degrading actinobacterium that was isolated from plastisphere formed on marine plastic debris. Polym Degrad Stabil. 2021. https://doi.org/10.1016/j.polymdegradstab.2020.109461.
44. Chen X, Zheng X, Fu W, Liu A, Wang W, Wang G, Ji J, Guan C. Microplastics reduced bioavailability and altered toxicity of phenanthrene to maize (*Zea mays* L.) through modulating rhizosphere microbial community and maize growth. Chemosphere. 2023;345:140444. https://doi.org/10.1016/j.chemosphere.2023.140444.
45. Suryadi Y, Susilowati DN, Fauziah F. Management of plant diseases by PGPR-mediated induced resistance with special reference to tea and rice crops. Microorg Sustain. 2019;13:65–110. https://doi.org/10.1007/978-981-13-6986-5_4.
46. Wang X, Cai X, Xu C, Wang Q, Dai S. Drought-responsive mechanisms in plant leaves revealed by proteomics. Int J Mol Sci. 2016. https://doi.org/10.3390/ijms17101706.
47. Marietou A, Roy H, Jorgensen BB, Kjeldsen KU. Sulfate transporters in dissimilatory sulfate reducing microorganisms: a comparative genomics analysis. Front Microbiol. 2018;9:309. https://doi.org/10.3389/fmicb.2018.00309.
48. Kushkevych I, Cejnar J, Treml J, Dordevic D, Kollar P, Vitezova M. Recent advances in metabolic pathways of sulfate reduction in intestinal bacteria. Cells. 2020. https://doi.org/10.3390/cells9030698.

Publisher's Note